Indian Journal of Science and Technology, *Vol 8(S7), 74–84, April 2015*
ISSN (Print) : 0974-6846
ISSN (Online) : 0974-5645

A Method for Calculating Aircraft Aerodynamic Loads Using Obtained Data from Flight Simulation

A. Gharibi[1*] and R. Khaki[2]

[1]Department of Aerospace Engineering, Amirkabir University of Technology, Tehran, Iran; ali.gharibi20@yahoo.com
[2]Aerospace Department of Shahid Sattari University of Air Science and Technology, Iran

Abstract

The loads applied to the structure of a plane are of two types, namely Inertia and aerodynamic. Aerodynamic loads result from the effects of the distribution of compressive forces acting on the exterior surface of the plane parts. These loads cannot be measured directly during the flight; however they are usually determined using numerical methods. In this research, the calculating of aerodynamic loads has been considered in all flight conditions. For this purpose, a training airplane has been chosen as a prototype, and also has been divided into small parts longitudinally. Furthermore, numerical solutions have been obtained under different effective parameters such as Mach numbers, angle of attack and control surfaces diversities as applying aerodynamic loads on the plane. Therefore, the magnitude of aerodynamic load which is applied to each part is found for a specific condition. Using resulted loads obtained from the numerical solutions under different applied parameters for each load, an equation has been derived to determine the applied aerodynamic load for each part through the least squares method. In order to obtain the variable values applied in the respective equation, flight simulation has been carried out for the training aircraft. To ensure the accuracy of simulation, its results have been validated with those of the flight tests. Then, the values of the variables used in the equations of the aerodynamic loads of different plane parts during the loop maneuver were recorded by flight simulation. Eventually, by substituting these values in the equations, the aerodynamic loads on different plane parts during the maneuver have been calculated. Results indicated that the proposed method for determination of the plane aerodynamic loads is appropriate.

Keywords: Aerodynamic Loads, Flight Simulation, Loop Maneuver, Flight Test, Regression Equations

1. Introduction

In order to determine the fatigue life, it is necessary to determine and to calculate the loads applied to the plane structure during its service span in the form of load spectra. To this end, numerous studies have been conducted to determine the forces applied on the structure of a plane during its life span.

Aerodynamic loads comprise a major part of these loads and many researchers have attempted to estimate and/or calculate these loads.

Nonlinear prediction of aerodynamic loads on lifting surfaces was carried out by Kandil[1] in 1974. Also, the nonlinear prediction of subsonic aerodynamic loads on wings and bodies at high angles of attack was carried out by Peiye. ZHU et al.[2] in 1980.

In 1990, Mark Drela[3] suggested another research approach for simultaneous wing aerodynamic and structural load prediction.

On a new method for prediction of scatter of loading spectra was suggested by Nagode et al.[4] in 1997. Cremona[5] made an effort for the optimal extrapolation of traffic load effects in 2001.

Fatigue life prediction and load cycle elimination during spectrum loading of composites were carried out by Schon et al.[6] in 2002. History of load spectra was used by Qingyuan et al.[7] in 2003 to calculate the probable distribution of local corrosion of constituent materials of aircraft parts due to fatigue.

In 2004 Karr et al.[8] demonstrated an algorithm for the calculation of loads applied to the plane structures under the worst gust conditions. In 2005, Heuler et al.[9]

**Author for correspondence*

studied the generation and application of standard load spectra and time history of loads for the calculation of fatigue life. Eduardo Salamanca et al.[10] in 2005 developed a method for the analysis of the bearing capacity of acrobatic planes against probable damage due to flight loads conformity. Timm et al[11] carried out studies on the characteristics of load spectrum through combining the modeling of its distribution in 2005. Qiu JU et al.[12] presented a study on the plane elevator aerodynamic loads in 2009.

Aerodynamic loads were carried out by Lee[13] in 2009 for F-16 hunting aircraft using parameters from flight data recorder during its service. He first obtained the loads applied to each part using strain meters installed on some plane parts and then calculated the aerodynamic loads by subtracting the inertia loads from the total applied loads. Using the aerodynamic loads and the parameters from the flight data recorder, he presented regression equation for the calculation of the plane aerodynamic loads at any time during the entire flight.

In our investigations, we have started studying the numerous methods to determine the aerodynamic loads applied to the airplane structure using the data found from flight simulation. In one of approaches, a training aircraft was selected as a prototype and numerical solutions have been obtained under different effective parameters such as Mach numbers, angle of attack and control surfaces diversities as applying aerodynamic loads on the plane. The airplane was longitudinally divided into small parts and the aerodynamic load applied to each part was found.

It is fairly difficult to determine the aerodynamic loads by numerical methods under all flight conditions or during the entire flight. Experimental methods are not economical either. Hence, it is necessary to specify a method for the estimation of aerodynamic loads applied to airplane parts under all flight conditions by using the aerodynamic loads obtained from numerical solutions.

To fulfill this, the regression equation for the calculation of aerodynamic loads applied to each part was specified under all flight conditions using the aerodynamic loads found from numerical solutions for different situations, the parameters of flight conditions and the least squares method.

To obtain the values of the variables used in the regression method, the dynamic simulation of the training aircraft was applied. Accuracy of the simulation was validated through the comparison of the simulation results of different maneuvers with those obtained from the flight tests during these maneuvers.

Finally, the loop maneuver was considered as a case for our simulation and the values of the variables used in the regression equations (of the members for this maneuver) were recorded. The aerodynamic loads applied to the airplane fuselage were then calculated.

2. Numerical Solution for Calculation of Aerodynamic Loads

Aerodynamic loads are of the results of the activities for the aerodynamic pressure distribution on the exterior surface of the plane parts. Appropriate pressure distribution cannot be measured by analytical methods under different conditions. However, the aerodynamic loads can be readily obtained using numerical solution of momentum and continuity equations approaches.

In this research, the aerodynamic loads have been calculated by numerical solution using the CFD. By which the aerodynamic model of the training aircraft was first developed. Then, the pressure distribution followed by the distribution of aerodynamic loads were obtained for nearly 300 flight conditions including different Mach numbers, angles of attack, control surfaces deflections, etc.

Figure 1 shows an example of the force distribution on various parts of an aircraft.

Since aerodynamic loads of an aircraft (under all flight conditions) are nearly impossible to obtain using numerical methods. Therefore, we have decided to consider regression equations for calculating the aerodynamic loads on various parts of the airplane obtained from software as well as other parameters applied under the same conditions.

3. Determination of a Suitable Equation for the Calculation of Aerodynamic Loads

The regression method has been used to specify the appropriate equation for the calculation of aerodynamic loads on members along the airplane. This method is a statistical approach to determine the relationship between one dependent variable and one or several other independent

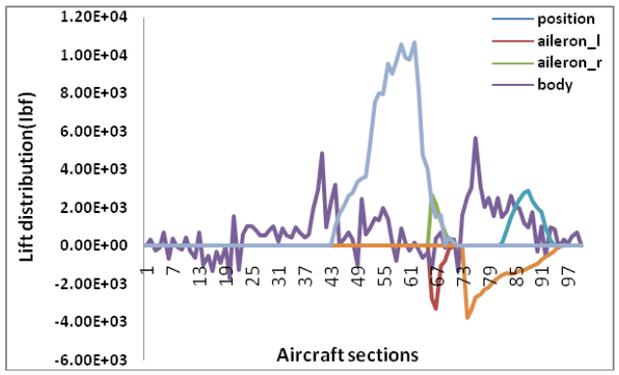

Figure 1. Example of force distribution on various parts of a plane during a flight.

variables. It has been applied to establish a relationship between the measured aerodynamic loads and the flight parameters used in the numerical solution. Such a relationship has led to the development of the "load equation" of that member.

The general form of the regression equation for aerodynamic loads on members is given below:

$$\text{Aerodynamic Load} = C_0 + C_1.x_1 + C_2.x_2 + \cdots + C_n.x_n \quad (1)$$

where, C0, …, Cn are the coefficients of the load equation and x1, …, xn are the flight parameters. The parameters which affect the calculation of aerodynamic loads are Mach number, angle of attack, angle of elevator, angle of rudder, and angle of ailerons.

Using coefficients determination of the given equation for each part, an appropriate equation was found for the calculation of the aerodynamic loads on all parts of the fuselage. For instance, the local shear aerodynamic loads equation of part 36 of the fuselage will be:

$$\text{Aerodynamic Load} = -186.9 + 7.73 * \alpha + 395.09 * M + 1.3 * dA - 5.26 * dE + 4.2 * dR + 11.6 * dF \quad (2)$$

Where, α is the angle of attack, M is Mach number, dA is the angle of ailerons, dE is the angle of elevator, dR is the angle of rudder, and dF is the angle of flaps.

In order to check the accuracy of the aerodynamic load equations, the loads found from the regression equations were compared with those of the numerical solutions. Figures 2 and 3 show examples of the relationship between the load distribution from the equations and that from the numerical solutions in two flight situations.

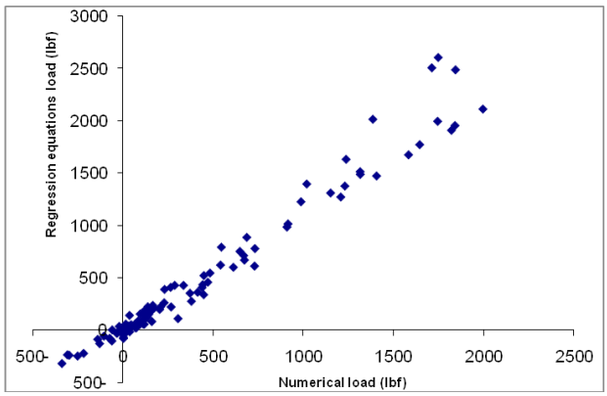

Figure 2. Relationship between aerodynamic loads from regression equations and numerical solutions with $\alpha = 5$ deg, M=0.597, dE=10deg, dA and dF=0 deg.

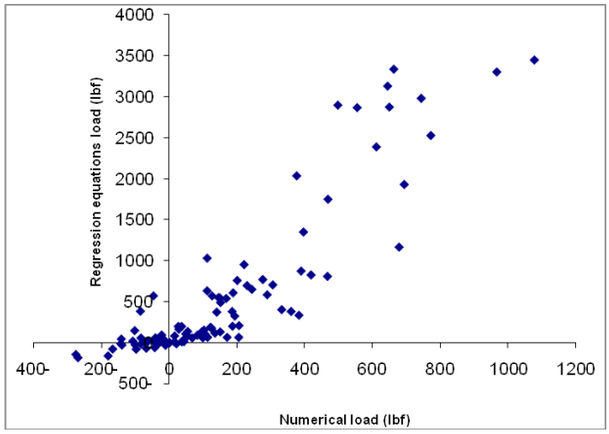

Figure 3. Relationship between aerodynamic loads from regression equations and numerical solution with $\alpha = 10$ deg, M=0.3, dF=11.43deg, dA and dE=0 deg.

Figure 4 shows the relationship of aerodynamic loads found from load equations and numerical solutions. The abscissa represents the distribution of aerodynamic loads from the numerical solution and the ordinate shows that from the load equations.

As the marked points (in the above Figures) approach the y=x line, it represents a better modeling of the aerodynamic loads by regression equations which means high precision of the load equations. As shown in Figures 2 and 3, the distribution of aerodynamic loads of the fuselage members from regression equations and that from the numerical solutions has a nearly linear relationship under similar conditions. But, as Figure 4 shows, the

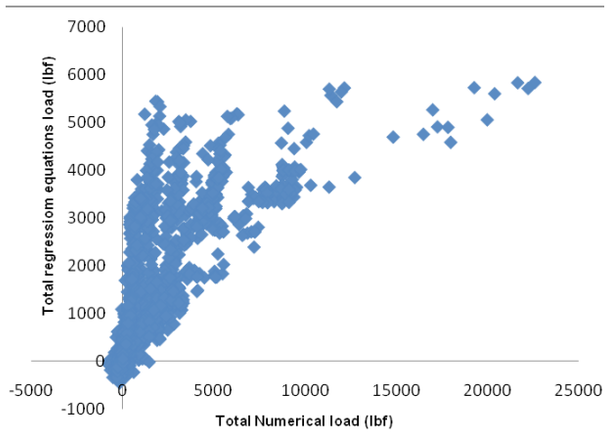

Figure 4. Relationship between all aerodynamic loads from regression equations and numerical solutions in different flight conditions.

relationship between all aerodynamic loads (from regression equations and numerical solutions) is not linear.

$$\text{Aerodynamic Load} = 22.68 * M^{\wedge 1.8} * \alpha^{\wedge 1.2} - 272.24 * M + 6.91 * dA + 6.31 * dE + 13.4 * dR + 31.36 * dF \quad (3)$$

In order to obviate the problems of regression equations, an equation was found using the least squares method for each airplane part so that the behavior of the equation and the aerodynamic loads found from numerical solutions under various conditions would become more balanced.

For instance, the equation for the calculation of aerodynamic loads of members 36 is:

In order to examine the precision of the derived equations, the load distribution obtained from these equations was compared to that from the numerical solution. Figures 5 and 6 show the relationship between these distributions.

Figure 7 represents the comparison between all aerodynamic loads obtained from the equations under different flight conditions and those obtained from numerical solutions under the same circumstances.

As Figures 5 and 6 shows, the relationship between the aerodynamic loads derived from the equations and those from the numerical solutions is linear. Also, the relationship between all aerodynamic loads obtained from the equations and the numerical solutions is nearly linear as illustrated in Figure 7.

A corresponding comparison of Figures 2 and 3 with Figures 5 and 6 shows that although the relationship between the aerodynamic loads derived from the regres-

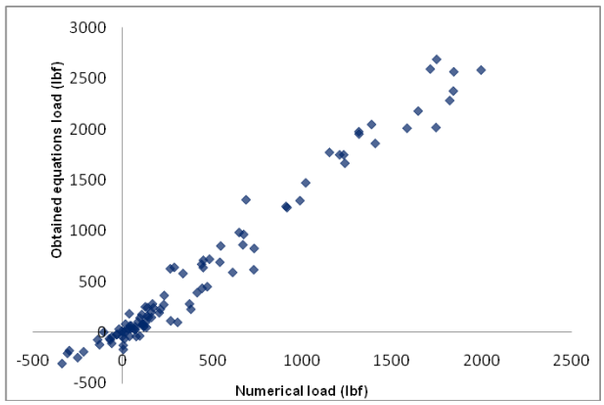

Figure 5. Ratio between aerodynamic loads of regression equations and numerical solution with $\alpha = 5\,\text{deg}$, M=0.597, dE=10deg, dA and dF=0 deg.

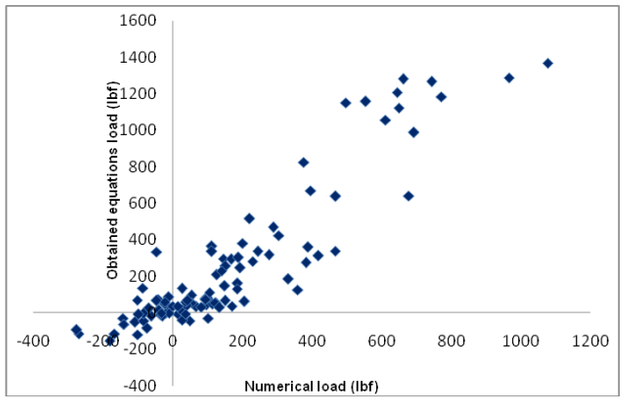

Figure 6. Ratio between aerodynamic loads of regression equations and numerical solution with $\alpha = 10\,\text{deg}$, M=0.3, dF=11.43deg, dA and dE=0 deg.

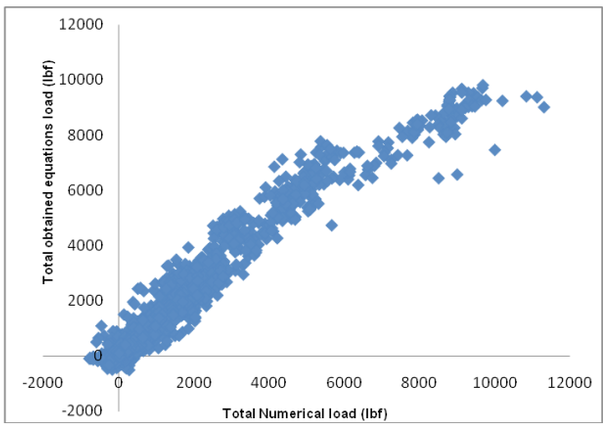

Figure 7. Relationship between all aerodynamic loads derived from regression equations and numerical solutions in different flight conditions.

sion equations and those from the numerical solutions is nearly linear, the aerodynamic loads obtained from the derived equations have a closer linear relationship with those obtained from the numerical solutions.

Moreover, it is evident from the comparison between Figures 4 and 7 that there exists an approximately linear relationship between the aerodynamic loads obtained from the derived equations and those from the numerical solutions in various flight conditions where as the relationship between the loads obtained from the regression equations and those from the numerical solutions are nonlinear. Thus, calculation of aerodynamic loads with the derived equations would be of higher accuracy and this is why we have used these equations to determine the aerodynamic loads on the airplane.

In this paper, Calculation of aerodynamic loads on the airplane by the flight simulation during the loop maneuver has been considered as a prototype and the simulation process and its validation have been described. The loop maneuver was run through simulation and the values of variables used in the respective equations were recorded substituting these values in the equations, the distribution of the aerodynamic loads on the plane was obtained.

4. Simulation Process

In order to run the dynamic or flight simulation by software, it is necessary to calculate the instantaneous stability derivatives for various flight conditions after modeling the nonlinear equations of the aircraft.

For this purpose, the required derivatives for the training aircraft were obtained by numerical method for different flight conditions with different parameters such as the sound velocity, altitude, angle of attack, control surfaces deflections, etc. These derivatives were arranged as a look-up table in the software so that it can calculate the desirable derivative under various flight conditions and situations through the interpolation process.

Having calculated the derivatives, the coefficients hence the aerodynamic forces and torques were obtained from simulation equations. The derived forces and torques were then used to obtain the linear and angular velocities, Euler angles, angle of attack and angle of sideslip.

In order to approximate the simulation conditions to the real ones, the inputs regarding the variations in the driving force and the relocation of control surfaces by the pilot via the joy stick, were also applied to the simulation software.

5. Simulation Validation

To verify the results obtained from the simulation, the parameters of the loop and Chandelle maneuvers, which are among the important flight maneuvers, were recorded during several real flights. Having run these maneuvers through simulation, the obtained data were compared with those from flight experiments.

The data from the simulation are presented in Tables 1 and 3 while those found from experiments are shown in Tables 2 and 4.

Table 1. Parameters of the loop maneuver derived from simulation

Condition	Air speed (kts)	Pitch angle (deg)	Mach Number	VLF (G)
1(start)	501.51	1.95	0.88	0.99
2	445.49	45.02	0.796	4.45
3	347.86	89.5	0.661	3.47
4	225.64	Invert 0.027	0.451	1.22
5	251.52	-45.01	0.5	1.82
6	328.93	-89.67	0.64	3.22
7	442.74	-45	0.79	3.87
8(End)	499.92	-1.06	0.85	0.98

Table 2. Experimental data of the loop maneuver

VLF (G)	Pitch angle (deg)	Air speed (kts)	Condition
1	0	500	**1(start)**
4.5	45	450	**2**
3.5	90	350	**3**
1.2	Invert 0	200	**4**
2	-45	250	**5**
3	-90	300	**6**
3.5	-45	440	**7**
1	0	500	**8(End)**

Table 3. Parameters of Chandelle maneuver derived from simulation

VLF (G)	Mach Number	Turn amount (deg)	Air speed (kts)	Condition
1	0.71	0	400	**1(start)**
3.51	0.68	45	363.9	**2**
2.88	0.61	90	310.9	**3**
1.9	0.52	135	271.7	**4**
1	0.39	180	200.9	**5 (End)**

Table 4. Experimental data of Chandelle maneuver

VLF (G)	Turn amount (deg)	Air speed (kts)	Condition
1	0	400	**1(start)**
3.5	45	360	**2**
3	90	300	**3**
2	135	250	**4**
1	180	200	**5 (End)**

Velocities found from simulation and flight experiment in different pitch angles are compared in Figure 8.

Figure 9 compares the Vertical Load Factors (VLF) derived from simulation and experiment in different pitch angles.

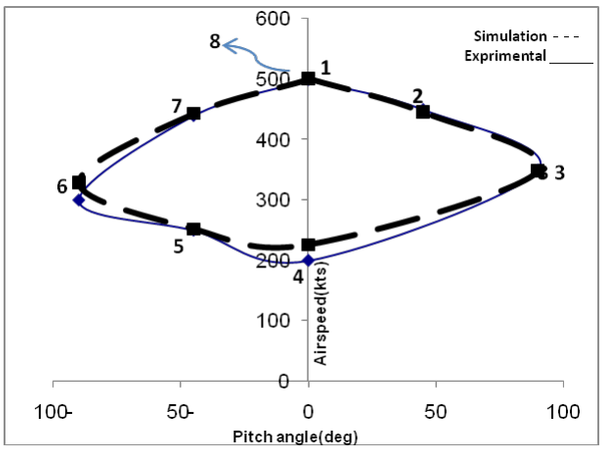

Figure 8. Comparison of simulation and experimental velocities in different pitch angles during the loop maneuver.

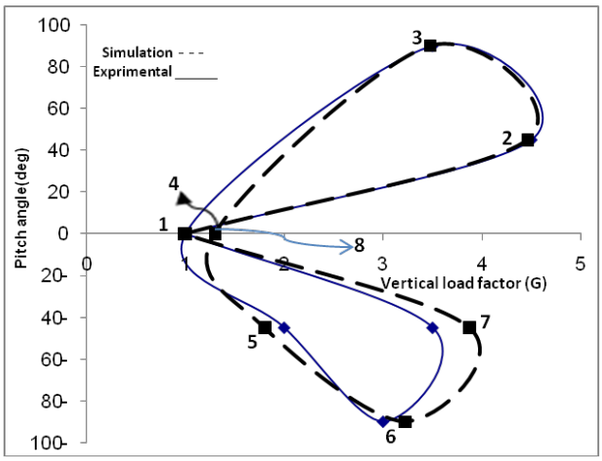

Figure 9. Comparison between VLF derived from simulation and experiment in different pitch angles.

Comparison of simulation and experimental velocities in different pitch angles during Chandelle maneuver is shown in Figures 10 and that of the vertical load factors in these angles in Figures 11.

Comparison of the experimental and simulated values of the VLF and velocity during the loop and Chandelle maneuvers reveals low simulation error (it is less than 13%).

Results show good accuracy of flight simulation and it can be concluded that they may be used to calculate the aerodynamic loads on an airplane.

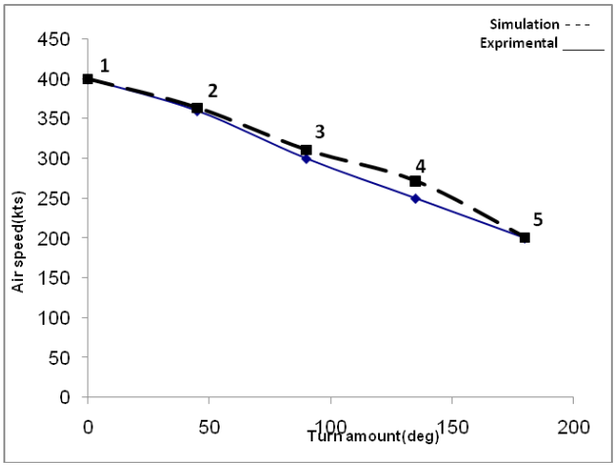

Figure 10. Comparison of simulation and experimental velocities in different pitch angles during Chandelle maneuver.

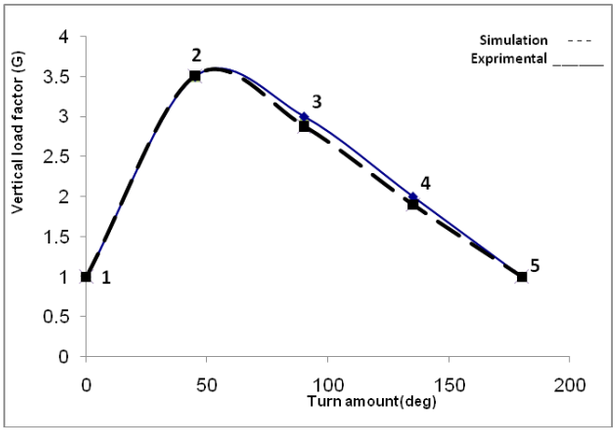

Figure 11. Comparison of VLF in different pitch angles during Chandelle maneuver.

6. Distribution of Aerodynamic Loads on an Airplane

In order to obtain the distribution of aerodynamic loads on an airplane, it is necessary to calculate the local shear dynamic loads of each part. To achieve this, the loop maneuver was done by flight simulation and the values of the variables used in the equations of the aerodynamic loads of the fuselage parts was recorded during the performing this maneuver. Values of these variables were recorded in short time intervals during the maneuver. Table 5 shows some of these values in different pitch angles.

Substituting the values in Table 5 in the related equations (of the calculation of the aerodynamic loads of the fuselage parts), the local shear aerodynamic load of each fuselage member was calculated for the corresponding pitch angle. Then, the distribution of aerodynamic loads of the fuselage was obtained.

Figures 12 to 15 present the distribution of aerodynamic loads on the fuselage in a number of pitch angles. The abscissa represents the 100 longitudinal parts of the fuselage and the ordinate shows the aerodynamic loads.

7. Interpretation of the results

During the loop maneuver, Mach number, angle of attack, angle of elevator and other relevant variables are varying continuously. Figures 16, 17 and 18 show respectively the variations of Mach number, angle of attack and elevator in different pitch angles during the loop maneuver.

For better analysis of the aerodynamic loads applied to the fuselage during the loop maneuver, this maneuver is divided into four quarters, namely 0 to 90 degrees pitch angle as the first quarter, 90 to 180 degrees (overturned) as the second, 180 to 270 degrees as the third and 270 to 360 degrees (zero position) as the fourth quarter. The aerodynamic loads applied to the aircraft in different situations are then compared during each quarter. Figure 19 shows the comparison of the distribution of the aerodynamic loads in the first quarter.

As the Figure shows, in a 60 degrees pitch angle, the maximum aerodynamic load is applied to the middle sec-

Table 5. Some values of the variables used in the equations (derived from simulation during the loop maneuver)

dF (deg)	dR (deg)	dA (deg)	dE (deg)	α (deg)	M	Pitch angle(deg)
0	0	0.07	-1.20	1.21	0.92	**0**
0	0	0.09	-17.02	7.32	0.87	**30**
0	0	0.02	-35.00	10.44	0.79	**60**
0	0	0.54	-35.00	10.40	0.68	**90**
0	0	1.00	-30.99	10.53	0.56	**120**
0	0	0.62	-24.99	10.53	0.47	**150**
0	0	0.17	-22.99	10.66	0.45	**180**
0	0	0.02	-23.00	10.82	0.48	**210**
0	0	0.95	-26.99	10.54	0.57	**240**
0	0	0.34	-35.00	10.27	0.69	**270**
0	0	0.07	-21.18	7.68	0.80	**300**
0	0	0.03	-10.43	6.33	0.86	**330**
0	0	0.06	-1.12	1.37	0.88	**360**

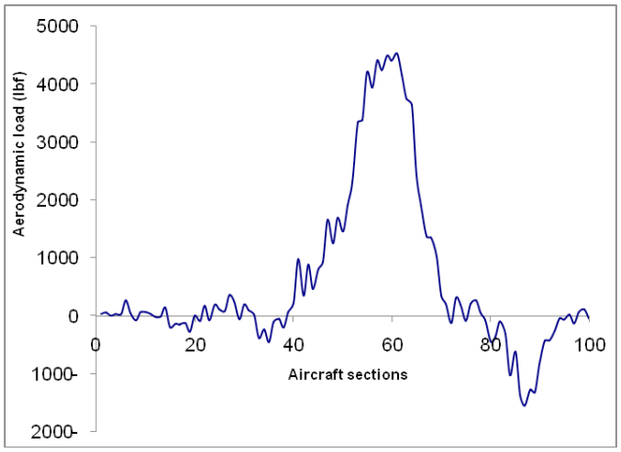

Figure 12. Aerodynamic load distribution of an aircraft in 30 deg pitch angle.

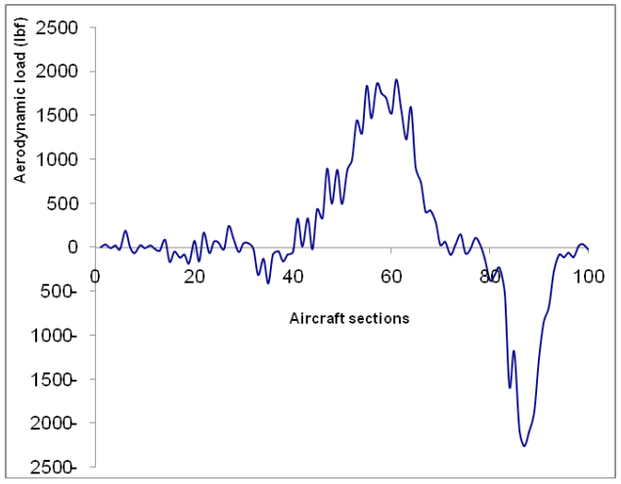

Figure 13. Aerodynamic load distribution of an aircraft in 150deg pitch angle

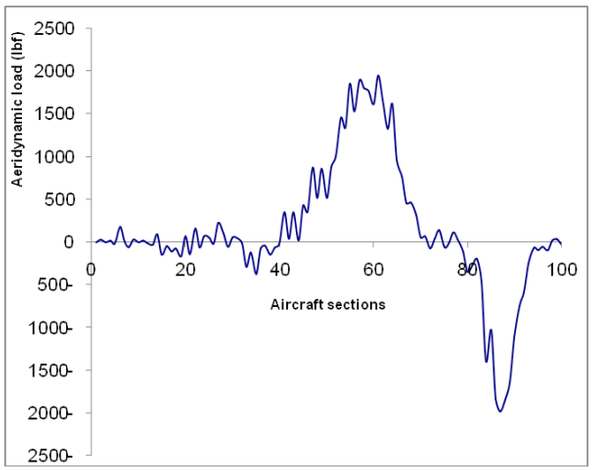

Figure 14. Aerodynamic load distribution of an aircraft in 210 deg pitch angle

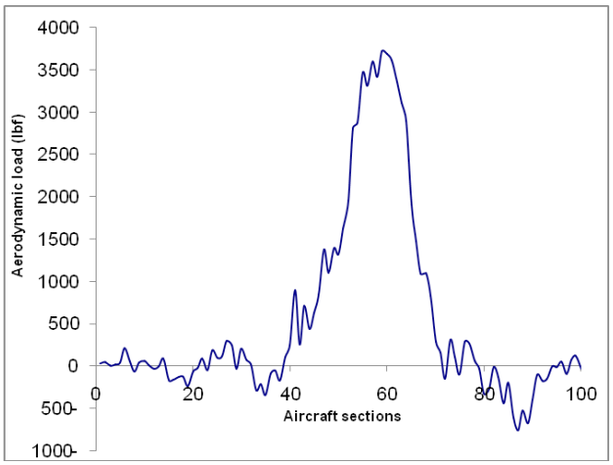

Figure 15. Aerodynamic load distribution of an aircraft in 330 deg pitch angle

tions of the fuselage where wings are connected. Also, in this situation, a great amount of aerodynamic load is reversely applied to the rear end of the fuselage where the elevator is connected. As Table 5 and Figures 16 and 17 shows, although Mach number has decreased compared to the two previous conditions, the angle of attack has increased and the angle of elevator (horizontal stabilizer) has also decreased.

The decrease in Mach number and angle of attack in the 90 degrees pitch angle has also caused a decrease in the aerodynamic loads applied to the middle sections of the fuselage compared to those applied in the 60 degrees

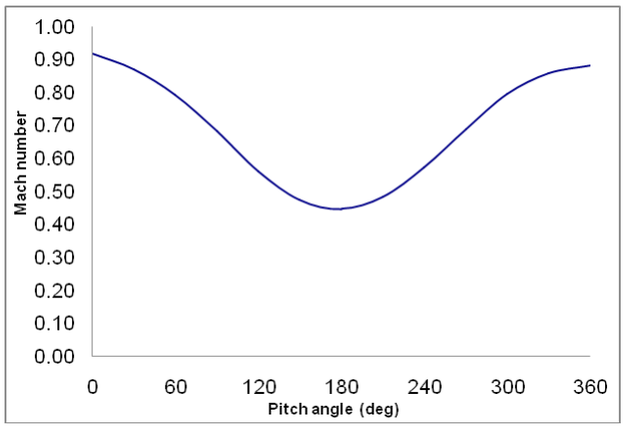

Figure 16. Variations in mach number in different pitch angles.

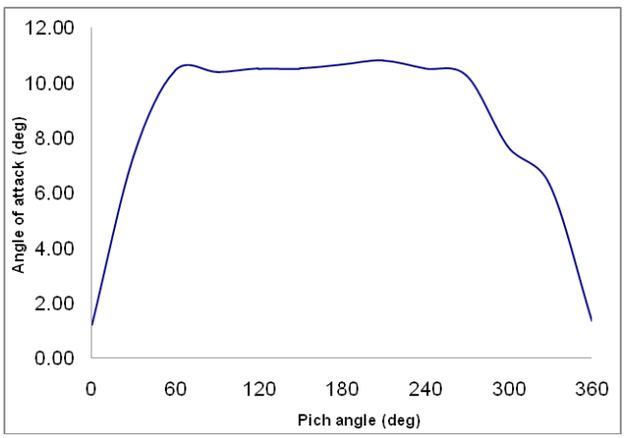

Figure 17. Variations in angle of attack in different pitch angles.

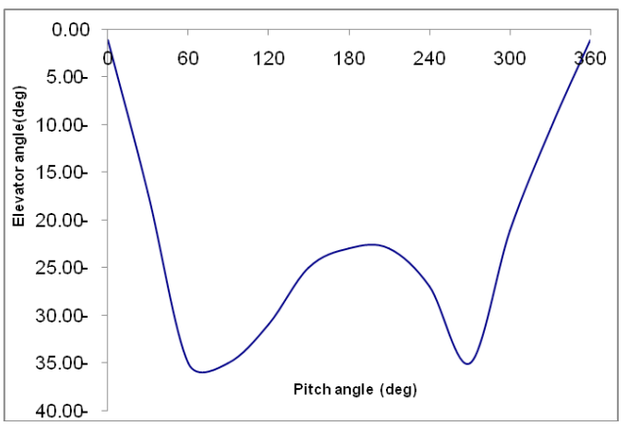

Figure 18. Variations in angle of elevator in different pitch angles.

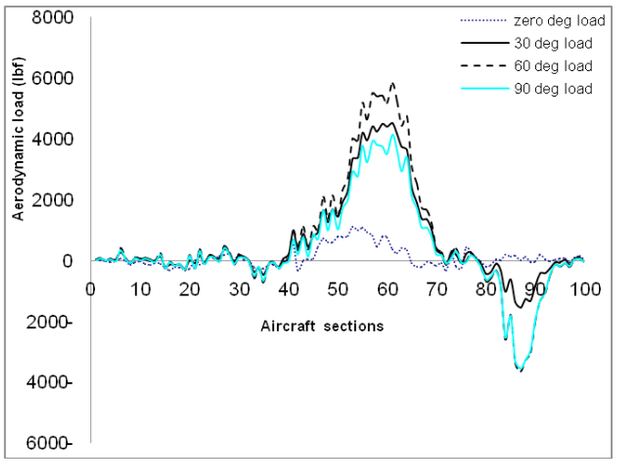

Figure 19. Comparison of the distribution of the aerodynamic loads in the first quarter of the loop maneuver.

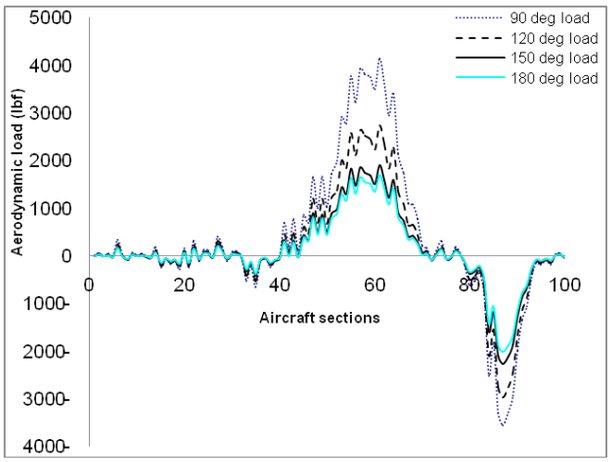

Figure 20. Comparison of the distribution of the aerodynamic loads in the second quarter of the loop maneuver.

pitch angle. No change in the angle of elevator in the two pitch angles of 90 and 60 degrees is the reason that the load applied to the rear end of the fuselage is constant.

Figure 20 shows the comparison of the distribution of the aerodynamic loads in the second quarter.

Considering Table 5 and Figure 20 as well as Figures 16 and 17, it is inferred that as the pitch angle increases during these situations, the angle of attack incurs a minor change of about 2% which is almost negligible but Mach number decreased considerably decrease (about 36%).

The minor increase in the angle of attack and the considerable decrease in Mach number cause the decrease in the aerodynamic loads applied to the middle sections of the fuselage. In this quarter of the maneuver, like in quarter one, the amount of the aerodynamic loads applied to the parts ahead of the wings connection section, is nearly constant for all situations. Also, as the pitch angle in this quarter increases, the aerodynamic loads applied to the rear parts decrease (increase in the reverse direction).

Figure 21 shows the distribution of the aerodynamic loads applied to the aircraft in the third quarter. As shown, the aerodynamic loads applied to the middle sections of the aircraft increase. Moreover, as the pitch angle increases, the aerodynamic loads applied to rear parts of the aircraft decrease (increase in the reverse direction).

Considering Table 5 and Figures 16, 17 and 18, it can be calculated that as the pitch angle in this quarter increases, the angle of attack decreases by about 3%, but Mach number increases by nearly 54%. Thus, the significant increase in Mach number in these conditions caused

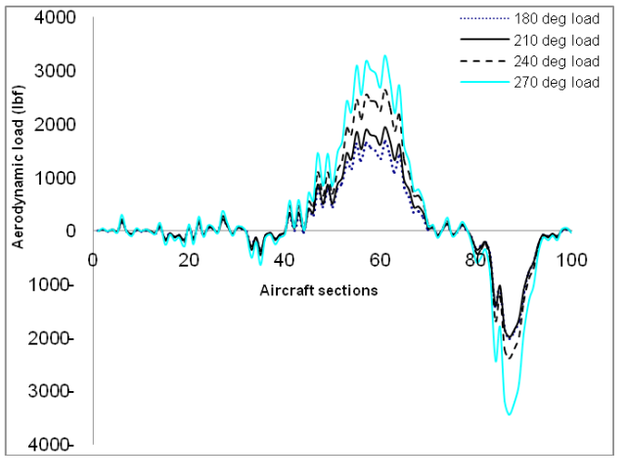

Figure 21. Comparison of the distribution of the aerodynamic loads in the third quarter of the loop maneuver.

the increase in the loads applied to the middle sections of the fuselage.

Decrease (increase in reverse direction) in the angle of elevator is the reason for the decrease in loads applied to the rear parts of the fuselage. Also, constant angle of elevator in 180 and 210 degrees pitch angles causes no variations in the loads applied to the rear end of the aircraft. In this quarter too, the loads applied to the front parts of the wings are constant in all conditions.

Figure 22 shows the comparison of the distribution of the aerodynamic loads applied to the aircraft in the fourth quarter of the loop maneuver.

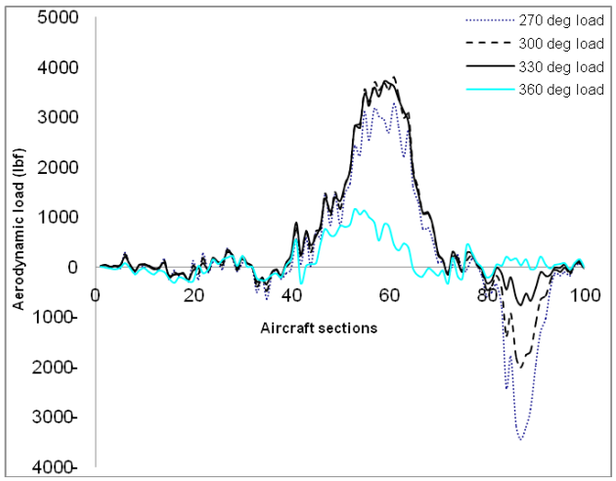

Figure 22. Comparison of the distribution of the aerodynamic loads in the fourth quarter of the loop maneuver.

Table 5 and Figures 16, 17 and 18 show that as the pitch angle increases, Mach number increases, the angles of attack decrease and the angle of elevator increases (decreases in the reverse direction). Increase in Mach number and in the angle of elevator in 300 and 330 degrees pitch angles, compared to those of the 270 degrees, leads to an increase in the aerodynamic loads on the middle sections of the fuselage in these two conditions. Significant decrease (almost 80%) in the angle of attack leads to decrease in the applied loads on the middle sections of the fuselage in the 360 degrees condition compared to those in the 300 and 330 degrees.

Also, with an increase in the pitch angle in this quarter, the decrease in the angle of elevator leads to the reduction of the applied loads on the rear parts.

Generally, it is evident that the decrease or increase in the angle of attack and Mach number has a major effect on the amount of the aerodynamic loads applied on the middle sections of the fuselage. Taking into account the considerable variation of the angle of attack during the loop maneuver, its role in the amount of the aerodynamic loads is more than that of Mach number.

In situations where the angle of attack during the maneuver is constant or has minor variations, the increase (decrease) in Mach number leads to an increase or (decrease) on the applied loads to the fuselage. The loads applied on the front parts of the fuselage during the maneuver are nearly similar and only have negligible differ in some situations.

Variation in the angle of elevator is an important factor in the loads variations in the rear end of the fuselage. However, these variations affect the loads applied to the front parts of the fuselage.

It is to be noted that the curves and calculations presented before were all to obtain the distribution of the shear aerodynamic loads along the fuselage. It is obvious that to obtain the amount of shear aerodynamic force (or bending moment) for a section, use has to be made of the sum of the shear loads (or bending moments) up to that section. Moreover, in order to calculate the bending moment, the total moment of shear loads of members up to that cross-section are used.

8. Conclusion

From our studies, we have observed that the relationship between the aerodynamic loads and those were found from the equations obtained using the numerical solution and using the least square method, respectively, is linear. Therefore, we concluded that the latter method can be considered as a suitable strategy for the calculation of the aerodynamic loads on airplanes.

The results which are obtained from the flight simulations have been compared with those recorded during the real flights under the similar conditions. The comparison showed a low error rate flight simulation. This error was less than 13% in our studies Thus, the parameters derived from flight simulation can be appropriate for the calculation of inertia loads on the fuselage.

The 89 percent variations (between the max and min values) of the angle of attack and the 52 percent variations of Mach number during the loop maneuver, indicated that the amount of aerodynamic loads applied to the middle sections of the fuselage depend, first, on the angle of attack and then on Mach number. Also, the amount of aerodynamic loads applied to the front parts of the fuselage is nearly constant during the maneuver.

The most important factor in the increase (decrease) in the aerodynamic loads applied to the rear parts of the aircraft is the increase (decrease) in the angle of elevator. Despite the variations in Mach number during the loop maneuver, the loads applied to the rear end of the aircraft remain constant due to the invariability of the angle of elevator.

Variations in the angle of ailerons during the maneuver were little and had no considerable impact on the applied loads.

List of Abbreviations

C0, C1, ….,Cn	coefficients of the load equation,
$X_{1,\ldots,}$ X_n	flight parameters,
α	angle of attack,
M	Mach number,
dA	angle of ailerons,
dE	angle of elevator,
dR	angle of rudder,
dF	angle of flaps,
VLF	vertical load factor,
Ibf	pound force,
G	unit of VLF,
Kts	Knots,
deg	Degree.

From our studies, we infer that the equations found by the least squares method and those from the flight parameters can be appropriate for the calculation of aerodynamic loads distribution. Though with finding the values of the variables of these equations through flight simulation, the aerodynamic loads applied to the fuselage of airplane can be calculated.

9. References

1. Kandil OA, Mook DT, Nayfeh AH. Nonlinear prediction of aerodynamic loads on lifting surfaces. J Aircraft. 1976; 13:22–8.
2. Zhu P, Shou W, Luo S. Nonlinear prediction of subsonic aerodynamic loads on wings and bodies at high angles of attack. Comput Meth Appl Mech Eng. 1981; 26(3):305–19.
3. Mark D. Method for simultaneous wing aerodynamic and structural load prediction. J Aircraft. 1990; 27(8):692.
4. Nagode M, Fajdiga M. On a new method for prediction of the scatter of loading spectra. Int J Fatigue. 1998; 20(4):271–7.
5. Cremona Ch. Optimal extrapolation of traffic load effects. Struct Saf. 2001; 23:31–46.
6. Schon J, Blom A. Fatigue life prediction and load cycle elimination during spectrum loading of composites. Int J Fatigue. 2002; 24:361–7.
7. Wang Q, Kawagoishi N, Pidaparti RM. Evaluation of the probability distribution of pitting corrosion fatigue life in aircraft materials. Acta Mech Sin. 2003; 19(3):247–52.
8. Karr C, Zeiler TA, Mehrotra R. Determining worst-case gust loads on aircraft structures using an evolutionary algorithm. Appl Intell. 2004; 20:135–45.
9. Heuler P, Klatschke H. Generation and use of standardized load spectra and load-time histories. Int J Fatigue. 2005; 27:947–90.
10. Salamanca HE, Quirz LL. *Superposition of flight loads for a probabilistic damage tolerance design for an acrobatic aircraft*. Int Aircraft Eng Aero Tech. 2005; 77(6):478–85.
11. Timm DH, Tisdale SM, Turochy RE. Axle load spectra characterization by mixed distribution modeling. J Transport Eng. 2005; 131:83–8.
12. Ju Q, Qin S. Research of aerodynamic load of horizontal tail. 4th IEEE Conference on Industrial Electronics and Applications; 2009. p. 1503–6.
13. Lee H. Advanced aircraft service life monitoring method via flight –by –flight load spectra. [PhD thesis]. Binghamton university state university of New York, 2009.